INSTITUTE OF PHYSICS PUBLISHING JOURNAL OF PHYSICS: CONDENSED MATTER

J. Phys.: Condens. Matter **16** (2004) 2585–2591 PII: S0953-8984(04)63146-8

# Pressure influenced combustion synthesis of $\gamma$- and $\alpha$-$Al_2O_3$ nanocrystalline powders

**O Ozuna**[1,3], **G A Hirata**[1,4] **and J McKittrick**[2]

[1] Centro de Ciencias de la Materia Condensada, Universidad Nacional Autónoma de México, Ensenada, BC, México, CP 22800, Mexico
[2] Department of Mechanical Aerospace Engineering and Materials Science and Engineering Program, University of California at San Diego, La Jolla, CA 92093-0411, USA

E-mail: hirata@ccmc.unam.mx

Received 8 May 2003
Published 2 April 2004
Online at stacks.iop.org/JPhysCM/16/2585
DOI: 10.1088/0953-8984/16/15/010

**Abstract**
Aluminium oxide nanocrystals have been prepared via a straightforward reaction, initiated at low temperatures (<300 °C), between aluminium nitrate and hydrazine. The initial pressure parameter is found to be responsible for the variations of the particle size (ranging from nanocrystalline to sub-microcrystalline) and for the resulting crystalline phase ($\gamma$- or $\alpha$-$Al_2O_3$) of these powders. The fibre-like morphology obtained for the as-synthesized $\gamma$-$Al_2O_3$ permits the synthesis of nanocrystalline $\alpha$-$Al_2O_3$ (~55 nm) even after a high temperature treatment at 1200 °C. The findings suggest a promising approach for controlling the size and crystal phase of the particles.

## 1. Introduction

Aluminium oxide (alumina, $Al_2O_3$) is a material with significant technological importance because of its large band-gap (~9.9 eV), high melting point (~2050 °C), chemical stability and excellent mechanical properties. Many structural modifications of aluminium oxides (e.g. $\gamma$, $\delta$, $\theta$ and $\alpha$) have been reported, $\alpha$-$Al_2O_3$ being the thermodynamically stable phase at normal pressure and temperature conditions. These materials are used as electronic substrates, bioceramics, structural ceramics and as supports for catalysts [1–3].

The main source of alumina is the Bayer process, which is used worldwide in the industrial processing of bauxites [1], but it has also been obtained through wet chemical methods such as the sol–gel technique [4], precipitation [5], combustion synthesis [6] and laser driven synthesis [7]. However, cheap and easy synthesis methods that can rapidly and

---

[3] Current address: Department of Physics and Astronomy, Arizona State University, Tempe, AZ 85287-1504, USA.
[4] Author to whom any correspondence should be addressed.

0953-8984/04/152585+07$30.00

continuously produce $\alpha$- or $\gamma$-$Al_2O_3$ of nanometre size, with large surface areas and well-defined composition and structure, have not been reported.

Several methods have been used to lower the phase transformation temperature to achieve nanocrystalline $\alpha$-$Al_2O_3$, because lowering this temperature prevents agglomeration and growth of the particles as well as reducing the energy input necessary for the process. For example, Messing *et al* [8–10] seeded bohemite gels with $\alpha$-$Al_2O_3$ and reported an acceleration in the formation kinetics but only a ∼50 °C depression in the transformation temperature was achieved. Sharma *et al* [11, 12] employed a surface modifier and seeding during the sol–gel process to lower the formation temperature of $\alpha$-$Al_2O_3$ from 1300 to $<1000$ °C; they also showed that the particle size of $\alpha$-$Al_2O_3$ can be tailored by controlling the pH of the modified alumina sol, thus reducing the particle size to the nano-range. Similarly, through a sol–gel route, it was reported that the nucleation temperature of $\alpha$-$Al_2O_3$ was lowered to 600 °C by seeding with particles with $\alpha$-$Al_2O_3$ structure; however, the complete $\gamma \rightarrow \alpha$ transformation did not occur until temperatures $>1100$ °C were reached [13]. Another approach for achieving nanocrystalline $\alpha$-$Al_2O_3$ used a surfactant induced fibre formation process to get fibres of $\gamma$-$Al_2O_3$ with a low sintering propensity that yielded nanocrystalline $\alpha$-$Al_2O_3$ even after high temperature processing [14].

Thus far, the only method really found capable of achieving $\alpha$-$Al_2O_3$ at really low temperatures is combustion synthesis. Generally, combustion synthesis is an excellent technique for preparing high temperature materials because of its low cost, high yield and the ability to achieve high purity and single- or multi-phase complex oxide powders in the as-synthesized state [15–17]. In this way the heat input needs only to reach an ignition temperature so that an exothermic, self-sustaining reaction takes place between precursors such as metal nitrates (oxidizers) and a carbonaceous fuel (reducer) [18]. In one such study, $\alpha$-$Al_2O_3$ powders with crystallite sizes between 0.2 and 0.8 $\mu$m were formed by igniting the precursors at 500 °C [6], but carbon contamination and there being no controllability of the particle sizes prevented further development of this technique.

In this work we present experimental results, which show that it is possible to synthesize nano- and sub-micro-alumina at very low ignition temperatures ($<300$ °C) using a combustion synthesis method [15] with some modifications that allow controllability of the particle morphology and size.

## 2. Experimental details

The structure of the powders was characterized using x-ray diffractometry (XRD) and transmission electron microscopy (TEM). Brunauer–Emmett–Teller (BET) $N_2$ adsorption experiments were used to measure the surface area.

$Al_2O_3$ powders were prepared using aluminium nitrate ($Al(NO_3)_3{\cdot}9H_2O$) and hydrazine ($N_2H_4{\cdot}H_2O$) as a reductive non-carbonaceous fuel. The reaction is exothermic and occurs at ∼280 °C (self-ignition temperature) according to

$$4Al(NO_3)_3(aq) + 15N_2H_4(aq) \rightarrow 2Al_2O_3(s) + 30H_2O(g) + 21N_2(g). \qquad (1)$$

The nitrate was dissolved in deionized water (∼25 ml) and then the hydrazine was added. (Hazard: hydrazine must be handled inside a glove box for safety reasons.) The vessel containing the mixture (250 ml Pyrex) was introduced into the reactor (2 l Parr 4522 pressure reactor) and then was tightly closed. A flux of 80 sccm of argon (Ar) was established for 15 min in order to create an inert atmosphere. At this time, the heating process began and the temperature was monitored via a type J thermocouple system inside the reactor. From this point three process conditions where used.

**Table 1.** Different procedure conditions and the resulting crystalline phases according to XRD experiments.

| Procedure Nos | Initial condition (at ∼110 °C) (MPa) | Condition before ignition (MPa) | Condition after completion (MPa) | Resulting phase (XRD) |
|---|---|---|---|---|
| 1 | Open | Open | Open | $\alpha$ |
| 2 | 0.2 | ∼1.3 | ∼5 | $\gamma + \alpha$ |
| 3 | 0.3 | ∼1.5 | ∼6 | $\gamma$ |

For clarity, the three different procedures are labelled accordingly (Nos 1, 2 and 3) and the specific conditions are summarized in table 1. The main difference is that in No 1 the exhaust valve was always open so the Ar pressure was not allowed to build up at all inside the reaction chamber. The chamber was continuously vented while being flushed with Ar until the temperature reached 200 °C; after that, heating continued until ignition (noticeable because of noise and a large amount of gas coming through the exhaust). In Nos 2 and 3, after the first 15 min of Ar flux, the exhaust valve was closed in order to allow the flowing Ar to pressurize the reactor chamber (at the initial condition value) and let the reaction take place in this closed environment. Before ignition, pressure had increased inside the reaction chamber but the greater increase was measured after completion of the reaction. This increase was due to the reaction forming gases inside the chamber. After this took place the exhaust valve was opened.

In all experiments, after the reaction occurred (which took about 1 s), the heater was turned off and Ar flow was re-established to avoid condensed water returning to the chamber. Although the heater was off, due to the exothermic nature of the reaction the temperature measured by the thermocouple increased to ∼330 °C before cooling to room temperature (although the *in situ* reaction temperatures could be much higher).

## 3. Results and discussion

The XRD patterns of the as-synthesized powders, obtained under the three different process conditions, are shown in figure 1. It is evident from figure 1(a) that using No 1, without pressurizing the reactor, direct synthesis of almost 100% $\alpha$-$Al_2O_3$ was achieved. This is in agreement with Patil *et al* [6], who formed $\alpha$-$Al_2O_3$ with nitrate and urea precursors. The XRD pattern from the powders formed using No 2 (figure 1(b)) shows the presence of both phases, the small broad peaks of $\gamma$-$Al_2O_3$ and the sharp peaks of $\alpha$-$Al_2O_3$. In figure 1(c) (No 3), the peaks correspond to $\delta$- and $\gamma$-$Al_2O_3$ crystalline phases. The broadness of these peaks implies very small crystals. The mean crystallite size, which was estimated using Sherrer's formula, is of the order of ∼25 nm. In addition, the BET method yielded specific surface areas of 7 $m^2\ g^{-1}$ for the sample prepared through No 1 and 104 $m^2\ g^{-1}$ for the sample obtained through No 3.

Preliminary experimental results show that various factors may affect the powder synthesis such as the heating ratio, fuel to oxidizer ratio and dilution of the reactant mixture, but the initial pressure is by far the most relevant. This may be explained as follows. At 135 °C both the $Al(NO_3)_3$ and hydrazine decompose, $Al(NO_3)_3$ freeing oxygen (O(g)) and hydrazine releasing ammonia ($NH_3$) and hydrogen ($H_2$) following equation (2):

$$2N_2H_4(g) \rightarrow 2NH_3(g) + N_2(g) + H_2(g). \qquad (2)$$

Decomposition results in gases with greater molar volume and capable of permeating the rest of the material inside the vessel. The enthalpy of reaction was determined as the difference

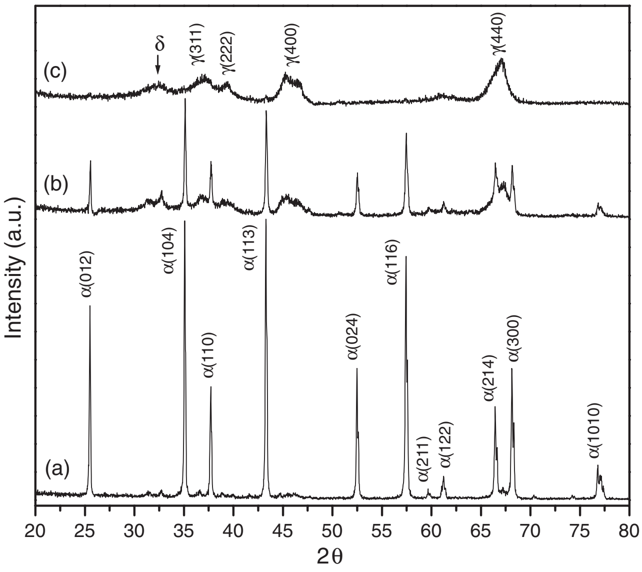

**Figure 1.** X-ray diffraction patterns of the as-synthesized $Al_2O_3$ powders obtained under different conditions: (a) No 1, atmospheric pressure (0.1 MPa); (b) No 2, under Ar pressure of 0.2 MPa; (c) No 3, under Ar pressure of 0.6 MPa.

between the formation enthalpies of the products and the reactants [19–22] and resulted as $\sim -9980$ kJ mol$^{-1}$ for both $\alpha$- and $\gamma$-$Al_2O_3$ synthesis. This value indicates that there is enough energy to account for the full crystallization of the product. The change in the initial pressure parameter, in procedures Nos 2 and 3, has a larger effect as an aid to the fuel permeation or filtration of gas through the pore space, which according to Holt [17] is a critical experimental parameter. Because the fuel permeates deeply inside the pore spaces, the combustion gases break up particles, stopping the agglomeration and crystallite growth mechanism, which tends to form larger crystallite sizes. Therefore an increase in pressure at the time the reaction occurs inside the closed chamber, where the gas evolved by the combustion reaction cannot be suppressed, results in smaller crystallite sizes.

As demonstrated by McHale *et al* [23], the structure, either $\gamma$- or $\alpha$-phase, depends directly on the surface area and therefore on the crystallite size. $\gamma$-$Al_2O_3$ has lower surface energy than $\alpha$-$Al_2O_3$, becoming energetically stable with respect to $\alpha$-$Al_2O_3$ at surface areas greater than 125 m$^2$ g$^{-1}$ and thermodynamically stable (lower entropy) at surface areas greater than 100 m$^2$ g$^{-1}$ at room temperature and 75 m$^2$ g$^{-1}$ at 527 °C. The BET values obtained for $\gamma$-$Al_2O_3$ (104 m$^2$ g$^{-1}$) and for $\alpha$-$Al_2O_3$ (7 m$^2$ g$^{-1}$) are in agreement with those values, providing additional experimental information about the difference in their surface energies.

Figure 2 shows the XRD patterns of different thermal treatments for the powders obtained through No 2. It is clear that transition ($\gamma$-, $\delta$-, $\theta$-) aluminas, grouped under the '$\gamma$' denomination, are stable up to 1100 °C and completely transform to $\alpha$-$Al_2O_3$ by 1200 °C. This result indicates the good thermal stability of the powders obtained by this method.

The formation of well-crystallized particles produced in this study is evident from the TEM image of the powders obtained through No 1, presented in figure 3(a). This shows an as-synthesized $\alpha$-$Al_2O_3$ microcrystal ($\sim$0.6 $\mu$m) surrounded by a small volume of nanocrystals ($\gamma$-$Al_2O_3$) of different sizes (5–20 nm). The large crystals are responsible for the narrow peaks observed in the XRD pattern in figure 1(a). Figure 3(b) shows the TEM image of

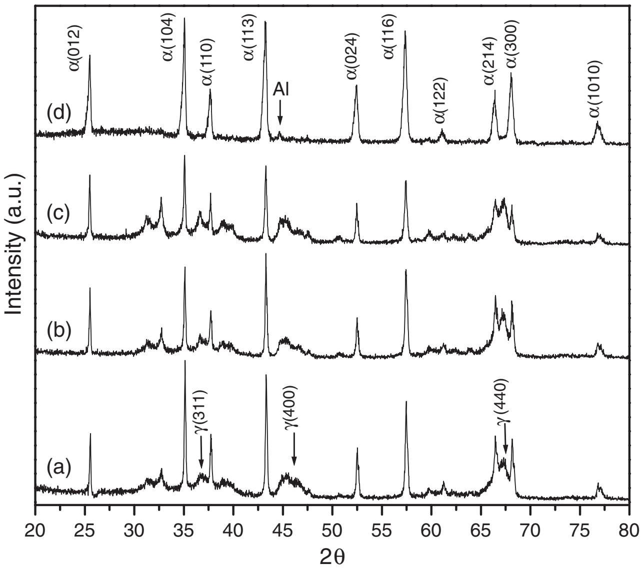

**Figure 2.** The XRD pattern of $Al_2O_3$ powder obtained under Ar pressure of 0.2 MPa (No 2) and heat treated in air for 2 h at various temperatures: (a) as-synthesized, (b) 900 °C, (c) 1100 °C (these three samples present a mixture of $\alpha$- and $\gamma$-phases) and (d) 1200 °C (this sample presents only the $\alpha$-phase). The peak labelled Al corresponds to aluminium and is due to the sample holder.

nanocrystalline (~55 nm) $\alpha$-$Al_2O_3$ achieved by heat treatment of the sample obtained by No 2 at 1200 °C for 2 h. In the correspondent XRD pattern (figure 2(d)), broad peaks are observed which result from the smaller size of the crystals (the mean crystallite size estimated using Sherrer's formula resulted in ~60 nm). Figure 3(c) shows the TEM image of the as-synthesized powders obtained through No 3; the crystallites appear as fibres having an average size of ~5 nm in width and ~40 nm in length. This is in contrast to other TEM micrographs of $\gamma$-$Al_2O_3$, which show spheres, platelets and a vermicular structure [24, 25]. Recently, Zhu *et al* [14] produced $\gamma$-$Al_2O_3$ with similar fibre morphology and demonstrated that this leads to a low sintering propensity. This explains the synthesis of nanocrystalline $\alpha$-$Al_2O_3$ even after a heating process, which usually results in agglomeration and uncontrollable crystallite growth.

## 4. Conclusions

Nanocrystalline $\gamma$-$Al_2O_3$ (crystallite size 5 nm × 40 nm) and microcrystalline $\alpha$-$Al_2O_3$ (~0.6 $\mu$m) powders were obtained at temperatures $<300$ °C by a pressure influenced combustion synthesis. $\alpha$-$Al_2O_3$ nanocrystals (~55 nm) can also be obtained by heat treatment (at 1200 °C for 2 h) of the fibre-like morphology $\gamma$-$Al_2O_3$, which showed very low sintering propensity. It was found that the initial pressure is the crucial parameter in determining the formation of $\alpha$-$Al_2O_3$ and/or $\gamma$-$Al_2O_3$ crystal phases in the combustion process. It is proposed that pressure induces the formation of $\gamma$-$Al_2O_3$ instead of $\alpha$-$Al_2O_3$ because it aids the permeation of the fuel mechanism, so at higher pressures the fuel filters through deeper inside the pore spaces; subsequently, when combustion occurs it breaks up particles leading to smaller crystallite sizes, where the surface dominates the crystal formation kinetics. Since $\gamma$-$Al_2O_3$ has lower surface energy it becomes the stable phase for these smaller crystals.

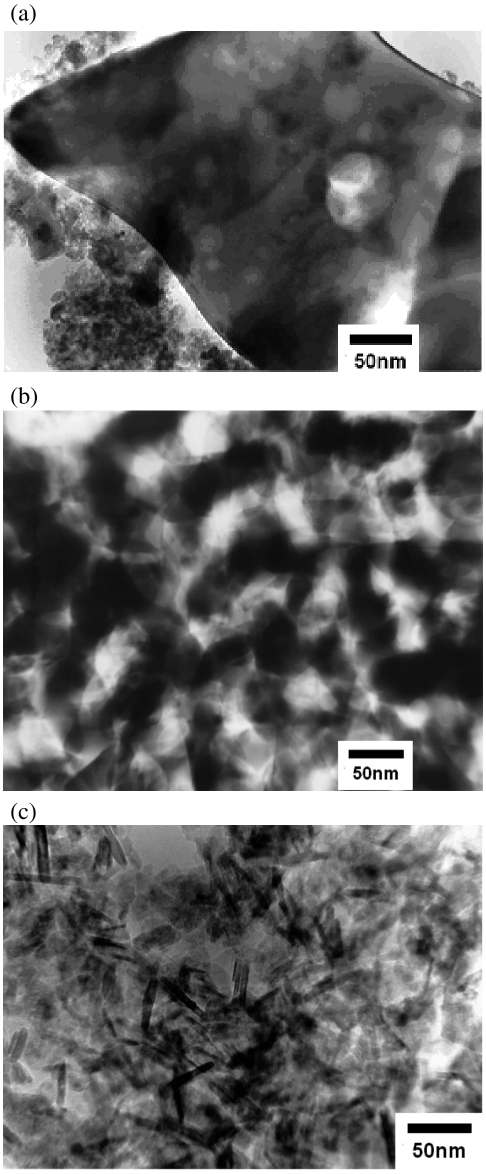

**Figure 3.** TEM micrographs of the powders obtained. (a) No 1 (0.1 MPa), as-synthesized. (b) No 2 (0.2 MPa), treated at 1200 °C for 2 h. These two micrographs show $\alpha$-$Al_2O_3$ crystalline phase. (c) No 3 (0.6 MPa), as-synthesized, showing only $\gamma$-$Al_2O_3$ nanocrystals.

Accordingly, the results obtained provide additional experimental evidence that differences in surface energy can favour the formation of a particular phase.

## Acknowledgments

We gratefully acknowledge the technical work performed by F Ruíz, E Aparicio, A Tiznado, E Medina, E Flores and G Vilchis. This work was partially supported by Conacyt-México (35971-U & 40128-F) and DGAPA-UNAM (IN105201).

## References

[1] McCauley J W and Haupin W 2001 *Encyclopedia of Materials: Science and Technology* ed K H J Buschow, R W Cahn, M C Flemings, B Ilschner, E J Kramer and S Mahajan (Oxford: Elsevier) p 127

[2] Christel P, Meuinier A, Dolot J, Crolet J, Witvolet J, Sedel L and Boritin P 1988 *Bioceramics: Material Characteristics Versus In Vivo Behavior* ed P Ducheyne and J Lemons (New York: Academic) p 523

[3] Burtin P, Brunelle J P, Pojolat M and Sostelle M 1987 *Appl. Catal.* **34** 225

[4] Yoldas B E and Parlow D P 1980 *Am. Ceram. Soc. Bull.* **59** 640

[5] Dudeney A W L, Ghani M A, Kelsall G H, Zhang L and Brit L 1991 *Ceram. Proc.* **47** 13

[6] Kingsley J J and Patil K C 1988 *Mater. Lett.* **6** 427

[7] Borcella E, Botti S, Giorgi R, Martelli S, Turtu S and Zappa G 1993 *Appl. Phys. Lett.* **63** 1345

[8] Messing G L, Kumagai M, Shellman R A and McArdle J L 1985 *The Science of Ceramic Chemical Processing* ed L L Hench and D R Ulrich (New York: Wiley) p 259

[9] Kumagai M and Messing G L 1984 *J. Am. Ceram. Soc.* **67** 230

[10] Bagwell R B and Messing G L 1999 *J. Am. Ceram. Soc.* **82** 825

[11] Sharma P K, Varadan V V and Varadan V K 2002 *J. Am. Ceram. Soc.* **85** 2584

[12] Sharma P K, Varadan V V and Varadan V K 2003 *J. Eur. Ceram. Soc.* **23** 659

[13] Youn H, Jang J W, Kim I and Hong K S 1999 *J. Colloid Interface Sci.* **211** 110

[14] Zhu H Y, Riches J D and Barry J C 2002 *Chem. Mater.* **14** 2086

[15] García R, Hirata G A and McKittrick J J 2001 *Mater. Res.* **16** 1059

[16] Munir Z A 1988 *Am. Ceram. Soc. Bull.* **67** 342

[17] Holt J B 1991 *Eng. Mater. HDB.* **4** 227

[18] McKittrick J, Bosze E J, Bacalski C F and Shea L E 1999 *Physical Properties of Combustion Synthesized Oxide Powders* ed F D S Marquis (Warrendale, PA: Minerals, Metals and Materials Society) p 139

[19] Cox J D, Wagman D D and Medvedev V A 1989 *CODATA Key Values for Thermodynamics* (New York: Hemisphere)

[20] Scott D W, Oliver G D, Gross W E, Hubbard W N and Huffman H M J 1949 *Am. Chem. Soc.* **71** 2293

[21] Mah A D 1951 *J. Phys. Chem.* **61** 1572

[22] ICSU-CODATA Task Group 1972 *J. Chem. Thermodyn.* **4** 331

[23] McHale J M, Auroux A, Perrotta A J and Navrotsky A 1997 *Science* **277** 788

[24] Reller A and Cocke D L 1989 *Catal. Lett.* **2** 91

[25] Reardon J, Datye A K and Sault A G 1998 *J. Catal.* **173** 145